

---

## Export of deep-sea hydrothermal particles, indigenous thermophilic microorganisms and larvae to the surrounding Ocean

Lesongeur Françoise<sup>1,2,3</sup>, Briand Patrick<sup>4</sup>, Godfroy Anne<sup>1,2,3</sup>, Crassous Philippe<sup>4</sup>, Byrne Nathalie<sup>2,3</sup>, Khripounoff Alexis<sup>4</sup>\*

<sup>1</sup> IFREMER, Ctr Brest, REM EEP, Lab Microbiol Environm Extremes, UMR6197, F-29280 Plouzane, France.

<sup>2</sup> CNRS, LM2E, UMR6197, F-29280 Plouzane, France.

<sup>3</sup> Univ Bretagne Occidentale, LM2E, UMR6197, Plouzane, France.

<sup>4</sup> IFREMER, Ctr Brest, REM EEP, Lab Environm Profond, F-29280 Plouzane, France.

\* Corresponding author : email address : [alexis.khripounoff@ifremer.fr](mailto:alexis.khripounoff@ifremer.fr)

---

### Abstract :

To assess the production and the export of particulate and biological material in deep-sea hydrothermal vents, four moorings with sediment traps and current meters were deployed for 24 days in the Azores Triple Junction (ATJ) region. They were deployed along an axis starting at the base of a hydrothermal vent chimney and ending 1000 m away. The particles sampled at the base of the chimney were characterized by high concentrations in total sulfur (16%) and iron (4%). The particle composition changed drastically with distance from the vent: the sulfur concentration decreased with an increase in clay components. Thermophilic microorganisms were successfully enriched from all the particle samples. Cultured strains were closely related to hydrothermal species, suggesting that viable hydrothermal vent microorganisms can be exported easily from one hydrothermal field to the open ocean. Fauna collected in the trap at the base of the chimney also included the hydrothermal mytilid species *Bathymodiolus azoricus* (prejuvenile prodissoconch late stage), larval or juvenile polychaetes and two vent gastropod species (*Shinkailepas* sp. and *Phymorhynchus* sp.). These organisms were not sampled by the others sediment traps. The most common taxa found in the traps off the vent were polychaetes, euphausiaceans and copepods (harpacticoids, nauplii and calanoids).

---

**Résumé :**

Exportation de particules, d'organismes thermophiles et de larves hydrothermales vers les grands fonds océaniques environnants. Pour évaluer la production et l'exportation de matières particulaires et biologiques des sources hydrothermales vers des grands fonds océaniques, quatre mouillages autonomes comprenant des pièges à particules et des courantomètres ont été déployés pendant 24 jours sur zone de jonction triple des Açores (ATJ). Ils ont été déployés le long d'un axe depuis la base d'une cheminée hydrothermale jusqu'à 1000 m de distance. Les particules, au pied de la cheminée, se caractérisent par des concentrations élevées en soufre total (16%) et en fer (4%). La composition des particules change radicalement en fonction de l'éloignement de l'évent hydrothermal: la concentration en soufre diminue avec une augmentation des composés de l'argile. Des micro-organismes thermophiles ont pu être cultivés sur tous les échantillons de particules. Les souches retrouvées sont étroitement liées aux espèces typiquement hydrothermales, ce qui suggère que ces micro-organismes viables hydrothermaux peuvent s'exporter facilement à partir d'un champ hydrothermal vers l'océan. La faune recueillie dans le piège à la base de la cheminée appartient à celle recueillie sur les sources hydrothermales de la zone comme l'espèce de mytilidé *Bathymodiolus azoricus* (dernier stade prodissoconque préjuvénile), des polychètes au stade larvaire ou juvénile et deux espèces de gastéropodes de source hydrothermale (*Shinkailepas* sp. et *Phymorhynchus* sp.) . Ces organismes n'ont pas été retrouvés dans les autres pièges à particules mouillés à plus grande distance de la cheminée. Les taxons les plus régulièrement trouvés dans ces pièges plus éloignés sont des polychètes, des euphausiacés et des copépodes (harpacticoïdes , nauplii et calanoïdes).

**Keywords :** Deep-sea hydrothermal vents, Particle flux, Hydrothermal microorganisms, Larvae, Regional index: North Atlantic, Mid-Atlantic Ridge, Azores Triple Junction

## 1. Introduction

---

The study of the material export by hydrothermal fields is now a significant part of deep-sea research due to the influence of vent fluids on the ocean's chemical balance (see Elderfield and Schultz, 1996). Large production of hydrothermal particulate material is dispersed in the deep ocean via fluid emissions and the precipitation of fine particles in the vent field and also via transport by neutrally buoyant hydrothermal plumes (Khripounoff et al., 2001). Hydrothermal vents also support singular ecosystem in which various type of "living particles" develops including prokaryotes, planktonic larval and juveniles of vent species (see review by Adams et al., 2012). Hydrothermal planktonic larvae can be very abundant close to vents (Khripounoff et al., 2001; Mullineaux et al., 2005) and these larvae show great temporal and spatial variation (Kim and Mullineaux, 1998; Metaxas, 2004). Possible occurrence of microbial communities living beneath active deep-sea hydrothermal vent systems has been suggested following observations of microbial communities in superheated hydrothermal emissions and inside sulfide chimneys (Schrenk et al., 2003). Recently, the presence of hyperthermophilic archaeal molecular signatures was reported from sub-seafloor sediments (Roussel et al., 2008). Nevertheless the existence of a deep subsurface biosphere does not exclude the possibility that thermophilic deep-sea vent microorganisms are transported on a small scale from one vent field to another in a manner similar to particle transport in open ocean waters. In 1990, the analysis of erupted rock fragments and plume seawater after the MacDonald Seamount eruption (Huber et al., 1990) demonstrated the occurrence of hyperthermophilic microbes. Hyperthermophilic microorganisms are therefore thought to be able to survive in cold oxygenated seawater and be transported in ocean waters.

The export of hydrothermal bacteria, metazoans and larvae appears to be the key process in the maintenance and the development of hydrothermal communities despite high habitat instability. Their transport off the hydrothermal field is closely linked to near-bottom currents and/or buoyant hydrothermal plumes several hundred of meters above the ocean bottom (Herring and Dixon, 1998; Mullineaux and France, 1995). These processes are responsible for the dispersal of vent species along mid-ocean ridges (Marsh et al., 2001). However, although a significant proportion of organisms must remain within their native habitat to maintain the local population assemblage, the magnitude of retention around the hydrothermal vent is still unknown (Khripounoff et al., 2008; Metaxas, 2004, Bailly-Bechet et al., 2008).

The originality of this study is to estimate the export of deep-sea vent material, both mineral and biological (e.g. particles, thermophilic microorganisms and metazoan larvae), using sediment traps to investigate hydrothermal organism supply to the surrounding ocean (Beaulieu et al., 2009). In this study, four moorings with sediment traps and current meters were deployed at various distances from the Eiffel Tower chimney in the Lucky strike vent field. Recovered particles were analyzed to determine their hydrothermal or pelagic origin, the presence of hydrothermal organisms and were checked for the presence of viable thermophilic prokaryotes using cell culture techniques and molecular methods to identify microorganisms.

## 2. Materials and methods

---

### 2.1. Study area

On the Mid-Atlantic Ridge, the Lucky Strike vent field (37°17'N, 32°17'W, 1600 m average depth) was chosen for this study (Fig. 1). This hydrothermal field was discovered in 1993 at the Azores Triple Junction (ATJ) (Langmuir et al., 1993). This area consists of a large central

lava lake surrounded by three volcanic cones. The chemical composition of the hydrothermal fluids at this site has been described by Colodner et al. (1993). Several translucent smokers are found on the sides of the volcanoes. Mussels are the dominant macrofaunal species and are distributed in patches of thousands of individuals (Desbruyères et al., 1991).

## 2.2. Sampling

Four moorings, composed of a frame with three sediment traps and a current meter, were deployed 24 days from 30 July to 25 August 2005 at the Lucky Strike field during the Exomar cruise (Fig. 1). These moorings can simultaneously sample particles in three sediment traps, each with different sampling bottle solutions. Each cylindrical-cone shaped sediment trap was made of epoxy fiberglass and had a sampling aperture of 0.07 m<sup>2</sup>, covered with a honeycomb baffle of 1 cm in diameter and 10 cm deep cells. Prior to deployment, the sampling bottles (3) in two traps on each frame were filled with sterile seawater for microbiological analyses. The bottles of the third trap were filled with filtered seawater containing sodium-borate-buffered formalin at a final concentration of 3% to prevent in situ microbial growth. This third trap was used only to analyze the particle composition and to calculate flux. After recovery, samples were stored in the dark at 4°C pending analyses. For each trap, the sampling periods were first during 7 days, then again 7 days and finally 10 days following a power regression model  $y = ax^{\beta}$

The first homemade triplicate sediment trap mooring (TS) was deployed by the ROV Victor, 3 m southeast of the active vent Eiffel Tower. The trap aperture was situated 1.5 m above the bottom (a.b.) for comparison of results with the previous studies at the same site (Khripounoff et al., 2000; Khripounoff et al., 2008). Three other triplicate sediment traps were deployed from the surface at respectively 100 m (T100), 300 m (T300) and 1000 m (T1000) from the South of the Eiffel Tower vent (Fig. 1) at 20 m a.b. This altitude was chosen to have sediment traps out of the resuspension sediment layer. The exact trap position on the bottom shown at the Figure 1 was obtained by acoustic positioning (BUC). The total flux data were analyzed following a power regression model  $y = ax^{\beta}$ .

Current meters RCM11 (Aanderra), positioned 5 m above traps TS and T1000, were equipped with a narrow range temperature channel (resolution: 0.006°C) and a pressure sensor. The current and its direction, as well as temperature and pressure, were recorded every 10 minutes.

## 2.3. Microbiological analysis: enrichment culture and strain identification

Back on board, particles recovered in each bottle of trap filled with sterile seawater were suspended and stored at 4°C in 50 ml serum vials under anaerobic conditions (N<sub>2</sub> gas phase). One month later, enrichment culture was performed using the following media: SMEYP medium in the presence of elemental sulfur at 90°C, GYPS medium (Postec et al., 2005) with and without elemental sulfur or thiosulfate at 60°C under N<sub>2</sub>:H<sub>2</sub>:CO<sub>2</sub> (90:5:5) gas phase and on a medium formulated for thermophilic methanogens at 80°C under a H<sub>2</sub>:CO<sub>2</sub>; (80:20) gas phase. All culture media were inoculated with particles in suspension at 2% and incubated from 16 h to several days. Microbial growth was checked daily using an Olympus BX60 phase contrast microscope.

Total DNA was extracted from positive enrichment culture using the Fast DNA kit for soil (Webster et al., 2003). Archaeal DNA was amplified using the primer A24F (5'-TTC CGG TTG ATC CTG CCG GA-3') and the reverse primer 1407R (5'-GAC GGG CGG TGW GTR CAA-3') or alternatively A23SR (5'-CTT TCG GTC GCC CCT ACT-3', position 257-234 on the *Thermococcus celer* 23S rRNA gene sequence). Bacterial DNA was amplified using

primers E8F (5'-AGA GTT TGA TCA TGG CTC AG-3') and the reverse primer U1492R (5'-GTT ACC TTG TTA CGA CTT-3') (Wery et al., 2002). PCR reactions were performed on a Robocycler Gradient 96 (Stratagene). PCR products were then checked on a 0.8% (w/v) agarose gel and directly cloned using the TOPO TA Cloning<sup>®</sup> kit (pCR2.1 vector), according to the manufacturer's instructions (Invitrogen<sup>®</sup>). Clone libraries were constructed by transforming *E. coli* TOP10F' cells. For each culture 10 clones were sequenced at the Biogenouest sequencing facility in Roscoff, France and partial 16S rRNA gene sequences of each unique phylotype were analyzed using the NCBI BLAST search program in GenBank (<http://www.ncbi.nlm.nih.gov/blast>) to determine their phylogenetic affiliations.

#### 2.4. Particle analysis and faunal sorting

Particles sampled with the trap bottles filled with formalin were sieved and the > 250  $\mu\text{m}$  fraction was examined under a dissecting microscope to sort, count and identify the organisms (particles smaller than 250  $\mu\text{m}$  contained only negligible proportions of nauplii and juvenile copepods). The < 250  $\mu\text{m}$  fraction was generally composed of few copepods and represented less than 5% of the total metazoan fauna in traps. The remaining particles without large fauna were rinsed with Milli-Q purified water (pH ~7), freeze-dried and weighed. Organic carbon concentrations were measured with a Leco WR12 elemental analyzer after removing carbonates with a 2 N HCl solution. Analysis of the chemical composition of particles was undertaken using EDAX DX-4i X-ray spectrometry. Standards were prepared in the laboratory from pure chemical compounds. Particles and standards were strongly compressed (5 t) to obtain a pellet of 3 mm in diameter with a very flat surface. The average accuracy of the analysis was 15 % for elements with a concentration of > 1%.

### 3. Results

---

#### 3.1. Currents and temperatures

Close to the Eiffel Tower vent, maximum current speed was  $18.6 \text{ cm s}^{-1}$ , and the mean speed was  $5.7 \text{ cm s}^{-1}$ . The general trend of the current direction fluctuated during the 24 days of the experiment. It was to the north during the first week, then to the southeast during the second week, and finally to the south (Table 1). We also observed also a significant tidal component recorded by the current meter close to the bottom. Recorded temperature varied between  $4.3^\circ\text{C}$  and  $5.6^\circ\text{C}$ . The highest temperatures were observed when current direction was between  $100^\circ$  and  $200^\circ$  (Fig. 2) corresponding to the periods when the trap was under the direct influence of the vent. The temperature anomalies recorded by the current meter represented an average of 16% of the recorded time, but they were not constant during the whole deployment period (Table 1).

At 1000 m to the South of the vent, maximum current speed was  $23.4 \text{ cm s}^{-1}$ , and the mean speed was  $6.8 \text{ cm s}^{-1}$ . The current direction always trended northeast-southwest and followed local bathymetry. A tidal signal was also recorded. The temperature variations were  $<0.6^\circ\text{C}$  and were not affected by vent emissions (Table 2).

#### 3.2. Total particle mass fluxes

At 3 m from the Eiffel Tower vents (TS), mean particle flux was  $601.9 \pm 220.5 \text{ mg m}^{-2} \text{ d}^{-1}$  (range  $380 - 870 \text{ mg m}^{-2} \text{ d}^{-1}$ ). At 100 m, 300 m at 1000 m away from the vent, the total particle fluxes were  $90.5 \pm 18.2 \text{ mg m}^{-2} \text{ d}^{-1}$ ,  $53.3 \pm 21.0 \text{ mg m}^{-2} \text{ d}^{-1}$  and  $38.9 \pm 4.6 \text{ mg m}^{-2} \text{ d}^{-1}$ , respectively (Fig.3). Mass fluxes showed high temporal variations during the 24 days of the

experiment (Fig.4). In the TS trap, fluxes increased over time and were highest during the last sampling period when the current direction was oriented from the vent towards the trap. Like TS, the T100 and T300 traps also showed the lowest flux during the first week. Only the trap at 1000 m did not appear to be influenced by the hydrothermal vent field (Fig. 4).

### 3.3. Particle composition

The main feature of the particle composition in the trap at the base of the vent was the dominance of sulfur (16%), the high concentration of iron (4%) and copper (1%) (Fig. 5A).. Organic carbon concentration increased from 5.8 to 10.5% over the study period in the TS trap and organic carbon with increased with particle flux (Fig. 6). The major chemical elements showed spatial fluctuations, especially sulfur, which was very abundant at the base of the chimney and decreased rapidly with distance from the vent. Fe showed a similar pattern. In contrast, the gradient was reversed for Si and Al, both constituents of clay, with relatively high concentrations at 1000 m and low concentrations at TS (Fig. 5). We observe the same trend in term of flux with a high flux of Ca at TS but not for Si and Al (Fig. 5B).

### 3.4. Thermophilic enrichment cultures and molecular affiliation of enriched microorganisms

From the TS and T100 particle samples, positive enrichment cultures with high cell densities ( $\geq 10^7$  cells /ml) were obtained after 16 h of incubation on SMEYP medium at 90° C. Growth was slower in T300 and T1000 particle samples. At 60°C, on GYPS sulfur and GYPS thiosulfate medium, TS (after 16 h) and T100 (after 24 h) particle samples respectively showed positive enrichment with high cell densities. For T300 particle samples, growth was better on the GYPS sulfur medium compared to GYPS with thiosulfate and there was no growth at 60° C on either GYPS media for T1000. No positive enrichment cultures were obtained on the methanogens medium (Table 3).

Using 16S rRNA gene sequencing, enriched species were identified. At 90°C on SMEYP medium, the cultivated species were all affiliated with genus *Thermococcus*. At 60°C on GYPS medium, species belonging to genera *Thermococcus*, *Caminiella* and *Desulfotomaculum* were recovered. When sulfur was replaced with thiosulfate, we only observed species related to the genera *Caminiella* and *Caloranoerobacter* (Table 4).

### 3.5. Fauna

Live animals were present in all sediment traps, but the faunal composition differed with distance from the vent (Table 5). Close to the vent, bivalve larvae in the prodissoconch last stage, belonging to the mytilid species *Bathymodiolus azoricus* (Comtet et al., 2000) were characterized by a uniform shell size suggesting that they were at the same stage of development. Larvae flux decreased during the last 10 day period, although the number of other organisms did not change (Table 5). Only a single bivalve larva of family Nuculidae was collected in the last trap sample. Polychaetes, primarily in larval or juvenile stages, were the dominant species in the trap. Adult gastropods, belonging to two vent species (*Shinkailepas* sp. and *Phymorhynchus* sp.), and copepods were also found in this TS trap. Benthic and planktonic organisms were collected at different developmental stages in the T100, T300 and T1000 traps. Euphausiaceans and copepods (harpacticoids, nauplii and calanoids) were the most common taxa. Only one *B. azoricus* larvae, the same species found in the TS trap, was observed only once in the T1000 trap.

## 4. Discussion

---

### 4.1. Particles emitted by the Eiffel Tower vent

Particle flux was equal to  $601.9 \pm 220.5 \text{ mg m}^{-2} \text{ d}^{-1}$  at the ST mooring at the base of the Eiffel Tower chimney and this value was 15 times higher than that recorded 1000 m away. Compared with the very high particle flux obtained at the Rainbow vents (average flux of  $6.9 \text{ g m}^{-2} \text{ d}^{-1}$  in Khripounoff et al. 2001), another ATJ vent field, the Lucky Strike vents seems to produce significantly less material and are comparable to the relatively shallow field Menez-Gwen found also in the ATJ (Desbruyères et al., 2001). Taken together, observations at various vent fields confirms that active vents that emit dark, particle-rich fluid, such as Rainbow, produce higher particle fluxes than the shallower vents such as Lucky Strike or Menez-Gwen which are characterized by translucent fluid (Khripounoff et al., 2008). Data collected at these vent fields confirms that the emitted material depends completely on the origin of vent fluid.

The particle flux collected close to the Eiffel Tower vent fluctuated greatly during the 24 days of the experiment and generally depended on the distance from the hydrothermal chimney (Fig. 3) following a power regression model  $y = ax^b$  ( $R=0.95$ ) and current direction (Fig. 4). At the base of the vent, temperature increased significantly when the current orientation trended south-southeast and placing the mooring downstream from the vent fluid. This favorable current which likely transported vent particles to the trap occurred 16% of the total sampling time, on average. For each sampling period, total flux intensity was linked with the duration of temperature anomalies (Fig. 4). This observation suggests that the large fluctuation in total flux can be attributed to current orientation. Vent emissions were not measured during the experiment and their role in the particle flux variations was unknown. The elemental composition of the particles sampled near the vent was characterized by high sulfur concentrations (S = 16%) and Fe (4%), which is the classic signature of hydrothermal fluid precipitation. Particulate sulfur content was slightly higher than that measured near Sintra, another vent of Lucky Strike field (11%) (Khripounoff et al., 2000) and similar to the sulfur concentration at Menez-Gwen, a shallower hydrothermal site in the Azores region (Desbruyères et al., 2001), and lower than the value reported from the hydrothermal Rainbow site (Khripounoff et al., 2001) or from East Pacific Rise vents (EPR) (Dymond and Roth, 1988). This comparison of different hydrothermal sites indicates that particle composition sampled close to hydrothermal chimneys basically reflects the variation in the composition of fluids emitted by vents.

### 4.2. Export of hydrothermal particles

Our results indicate that vent particle export generally depends on the speed and the direction of local currents as the model of Bailly-Bechet et al., 2008) which predicts that bottom currents often dominate all other factors in the larval dispersal. Currents were favorable for vent particle transport in all the sediment traps during several periods. Sulfur, an element originated primarily from vent fluids, is a good indicator of hydrothermal particle origin: it is abundant in hydrothermal particles and rare in the pelagic-origin particles. Sulfur concentration showed large spatial fluctuations during this experiment: 16% close to the vent and, 8.6% at 100 m, 2% at 300 m and  $<0.5$  at 1000 m. Using this data, we can assume that, at a distance of 100 m, half of the particles had hydrothermal origin and the other half part was composed of pelagic material. At 300 m, this percentage dropped to only 13% of hydrothermal particles in the total flux. The very low sulfur concentration in particles and the low total flux measured at 1000 m, indicate that the vent material rarely reaches this

distance. Our results suggest that, despite frequently favorable current directions, the amount of vent material decreases with the distance from the chimney due to rapid particle settlements on the bottom. For Baily-Bechet et al., 2008) When bottom currents are very slow, particles or larvae motion is upwards with vertical slopes favor retention of larvae because larval initial trajectory is nearly parallel to the smoker wall, which increases the chances to settle.

Material flux from the chimney is also massively diluted as a consequence of its dispersal from a vent in the surrounding ocean. At the Rainbow vent field, Khripounoff et al. (2001) reported the presence of hydrothermal particles in a trap situated 500 m from the vents but not in the traps located at 1000 m. Considering our results, direct advective transport by currents from local sources does not appear to be the main mechanism of hydrothermal large particle export to the open ocean because particles settle too quickly or are too diluted. The plume created by the thermal gradient, which may hold very small (few  $\mu\text{m}$ ) and concentrated hydrothermal particles such as eggs, microorganisms or light weight floating larvae floating (some zooplankton can drift for several days) over several kilometres (Adams et al, 2012). The mechanism of hydrothermal material dispersal at a larger scale (more than 100 km) is still unknown.

The flux measured in the T1000 trap ( $39 \text{ mg m}^{-2} \text{ d}^{-1}$ ) was higher than the pelagic particle flux measured for one year in the vicinity of the Rainbow vent field ( $11 \text{ mg m}^{-2} \text{ d}^{-1}$ ) in 1997 (Khripounoff et al. 2001) and at the Lucky Strike field in 1994 ( $8 \text{ mg m}^{-2} \text{ d}^{-1}$ ) (Khripounoff et al., 2000 and 2001) . However, all fluxes measured in the ATJ area are particularly weak compared to data recorded in the Atlantic Ocean (Auffret et al., 1996). The ATJ area, with a pelagic flux lower than  $50 \text{ mg m}^{-2} \text{ d}^{-1}$  is characteristic of an oligotrophic area.

#### 4.3. Biological supply

The hydrothermal vents may export not only mineral material but also living organisms, such as microorganisms and small animals. Both thermophilic Bacteria and Archaea originating from deep-sea vents were successfully cultivated from trap samples. Species belonging to genus *Thermococcus* were enriched from all particle samples (TS to T1000). Species from this group are thermophilic chemoorganotrophic anaerobes and are present in almost all hot ecosystems, whether they are continental, shallow marine waters or deep-sea vents. In addition, they are known to tolerate long-term storage at low temperatures even in oxic conditions (Erauso et al, 1993). Other bacterial species were detected, all belonged to the Firmicutes and closely related to species that have been isolated from deep-sea hydrothermal vents. Of the cultured bacteria, we found species belonging to genus *Caminicella* (enriched in TS, T100 and T300 particle samples), *C. sporogenes* is an anaerobic fermentative species first isolated from the EPR at  $13^\circ\text{N}$  (Alain et al., 2002). Species belonging to this genus have also been sampled from a hydrothermal chimney at the Rainbow vent field (Postec et al., 2007). *Caloranaerobacter azorensis*, found in TS and T300 traps, is a thermophilic anaerobic fermentative species that has been isolated from the Lucky Strike vent field (Wery et al., 2001). Microorganisms belonging to genus *Desulfotomaculum* were enriched from TS and T100 particles samples. Species of this genus are sulfate-reducing bacteria that have been isolated from various anaerobic ecosystems and this genus includes thermophilic species (Haouari et al., 2008; Kaksonen et al., 2006).

Culturability of deep-sea vent microorganisms weakens with distance and only *Thermococcus* species were recovered in the T1000 sediment trap. This low culturability may be due to the decrease in hydrothermal particle concentration with the distance from the vent and, consequently, a decrease in the number of hydrothermal microorganisms recovered in the traps. However, the low recovery rate may also be related to the ability of organisms to

survive in cold oxygenated water: species belonging to genus *Thermococcus* are known to tolerate oxygen at low temperatures *in vitro*, while sulfate-reducers such as *Desulfotomaculum* are less resistant to oxygen. Methanogens are rapidly inhibited by oxygen and their culture requires very strict anoxic techniques. The failure to enrich methanogen species can be also explained by recent results that report an absence of methanogen sequences in all Lucky Strike vent field samples analyzed using multiplexed barcoded pyrosequencing (Flores et al, 2011). Although, the presence of viable thermophilic prokaryotic cells in all sediment traps is consistent with possible dispersal of some hydrothermal species in the surrounding oceanic waters. Although microbial diversity of hydrothermal vent chimneys has been largely investigated in the past few years, the colonization processes of new hydrothermal sites remain unclear. McCliment et al. (2006) hypothesize that nascent chimneys are first colonized by chemolithoautotrophic microorganisms such as Ignococcales and that the next colonizers are *Thermococcus* species. Finally, Thermococcales sequences are dominant in a molecular inventory of young hydrothermal spires from Lucky Strike and TAG fields (Byrne et al., 2009). Together these data strongly suggest that Thermococcales are the first to colonize deep-sea vent chimneys (Byrne et al., 2009).

The hydrothermal metazoan fauna sampled by the sediment traps was abundant but not diverse. Its density varied with time and depended on sampling location. Close to the hydrothermal vent, the densities of postlarvae bivalves and gastropods sampled by the sediment trap were similar to the results obtained with the same method in this area by Khripounoff et al. (2008). As observed for microorganisms and particles, there was a rapid decrease in hydrothermal organism density in the traps with increasing distance from the hydrothermal chimney (Table 5). No hydrothermal fauna were sampled at distance greater than 100 m from the chimney with the exception of one *B. azoricus* larvae bivalve shell in the T1000 trap. However, sediment traps are known to be selective, and they do not accurately predict plankton or larval concentration (Beaulieu et al., 2009). Because sediment traps only collect settling material, free-swimming larval stages will be underrepresented in trap collectors. Although other free-swimmer fauna such as planktonic species can be collected by traps, the sampling of these organisms is only qualitative and sediment traps are not appropriate for the study of their distribution. Despite these limitations, sediment traps remain useful for a qualitative study of larvae behavior (Adams and Mullineaux, 2008). In this study, the typical hydrothermal fauna sampled in the trap moored close to the Eiffel Tower chimney was characterized by abundant numbers of prejuvenile prodissoconch late stage of *B. azoricus* and adult gastropods as described by Khripounoff et al., (2008) in the same hydrothermal field. These animals sampled in the trap at the base of the chimney probably had not left their natal site. This suggests that chemical or/and hydrodynamic larval retention factors favor their development over several weeks in the same location. Adams and Mullineaux (2008) noted that, on a scale of about 1.6 km, the hydrothermal gastropod supply appears to be influenced by direct transport from local sources. Spatial or temporal variation in larval density may also have contributed to the observed fluctuation in benthic hydrothermal faunal abundance. Other small organisms, such as polychaetes, were found in the sediment traps moored close to the vent.

The organisms that dominate the background pelagic flux belonged mainly to zooplankton fauna. The density of copepods in the T1000 pelagic trap was higher than in the traps deployed closer to the vent. Several studies have demonstrated that zooplankton abundance often increases near hydrothermal fields presumably due to the higher food supply (Herring and Dixon, 1998; Mullineaux and France, 1995). Conversely, other observations suggest that the toxicity of the water prevents the colonization of several zooplankton taxa close to hydrothermal chimneys (Burd and Thomson, 1995; Khripounoff et al., 2008). It is likely that the trap position directly downstream from vent emissions is unfavorable to the permanent presence of several species near the hydrothermal vents and thereby may explain the decrease in plankton close to the Tower Eiffel chimney.

While both metazoan and microorganisms associated with vent particles can be exported at short distances from the vents, only microorganisms appear to be exported on a larger scale by a direct advective transport. The results presented in this work do not preclude rare, long distance dispersal events of few individuals that would ensure the colonization of new vents. However, transport by hydrothermal plumes and eddy currents are more plausible hypotheses to explain the dispersal of small floating mineral or living particles (Adams et al., 2011). The pathway of larval transport, via advective transport along the ridge axis may thus be an alternative mechanism of dispersal.

Hydrothermal particle production by the Eiffel Tower vent (Lucky Strike field-ATJ) and particle export to the open ocean are mainly controlled by current direction, depending on the topography of the rift valley (Baillly-Bechet et al., 2008). At 100 m from the chimney, the proportion of hydrothermal particles was about half that collected close to the vent. The lack of hydrothermal particles at 1000 m, south of the vent, demonstrates that large particles, which are able to settle very rapidly on the bottom, were not found very far from the emission site. Fluxes of hydrothermal biological material also decreased with distance from the vent. The most common hydrothermal metazoan fauna found in the trap deployed close to the chimney were bivalve larvae and adult snails. However, like the hydrothermal mineral particles, the presence of fauna rapidly dropped being replaced by pelagic zooplankton when the distance from the vent increased. Thus, the lack of larvae in traps away from the vent could be due to a horizontal gradient in larval supply (driven by larval behavior) or it could be due to the vertical gradient in planktonic larval concentration or are able to settle very rapidly on the bottom. The main mechanism of large hydrothermal particle export to the open ocean does not seem to be due to direct advective current transport. However, the presence of some viable thermophilic prokaryotic cells in the trap at 1000 m from the vent suggest that some hydrothermal microorganisms are able to survive in cold oxygenated water and are exported from one vent site to another, thereby ensuring colonization of new hydrothermal sites.

## Acknowledgments

---

We would like to thank the captain and crew of the N/O Atalante and the ROV Victor team. The scientific and technical staffs participating in the EXOMAR cruise are also warmly acknowledged. We are grateful for comments and suggestions by F. Pradillon.

## References

---

- Adams D.K. & Mullineaux L.S. 2008.** Supply of gastropod larvae to hydrothermal vents reflects transport from local larval sources. *Limnology and Oceanography*, **53**: 1945-1955.
- Adams D.K., McGillicuddy D.J., Zamudio L., Thurnherr A.M., Liang X., Rouxel O., German C.R. & Mullineaux L.S. 2011.** Surface-generated mesoscale eddies transport deep-sea products from hydrothermal vents. *Science*, **332**: 580-582.
- Adams D.K., Arellano S.M. & Govenar B. 2012.** Larval dispersal: Vent life in the water column. *Oceanography*, **25**: 256-268.
- Alain K., Pignet P., Zbinden M., Quillevere M., Duchiron F., Donval, J.P., Lesongeur F., Raguene G., Crassous P., Querellou J. & Cambon-Bonavita M.A. 2002.** *Caminicella sporogenes* gen. nov., sp. nov., a novel thermophilic spore-forming bacterium isolated from an East-Pacific Rise hydrothermal vent. *International Journal of Systematic and Evolutionary Microbiology*, **52**: 1621-1628.

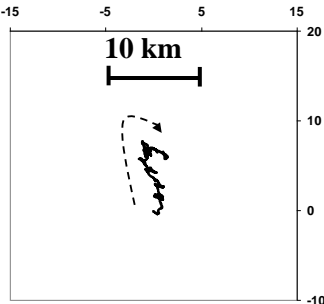
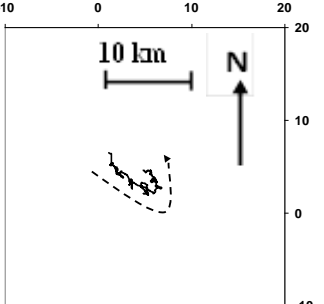
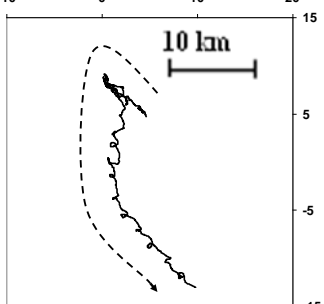
- Auffret G., Richter T., Reyss J.-L., Organo C., Deloule E., Gaillard J.-F., Dennielou B., Muller C., Thomas B., Watremez P., Grousset F., Boelaert A., Cambon P. & Etoubleau J. 1996.** Enregistrement de l'activité hydrothermale dans les sédiments de la dorsale médio-atlantique au Sud des Açores. *Comptes Rendus de l'Académie des Sciences de Paris, Série II*, **323**: 583-590.
- Bailly-Bechet M., Kerszberg M., Gaill F. & Pradillon F. 2008.** A modeling approach of the influence of local hydrodynamic conditions on larval dispersal at hydrothermal vents. *Journal of Theoretical Biology*, **255**:320-331
- Beaulieu S.E., Mullineaux L.S., Adams D.K. & Mills S.W. 2009.** Comparison of sediment trap and plankton pump for time-series sampling of larvae near deep-sea hydrothermal vents. *Limnology and Oceanography Methods*, **7**: 235-248.
- Burd B.J. & Thomson R.E., 1995.** Distribution of zooplankton associated with the Endeavour Ridge hydrothermal plume. *Journal of Plankton Research*, **17**: 965-997.
- Byrne N., Lesongeur F., Bienvenu N., Geslin C., Alain K., Prieur D. & Godfroy A. 2009.** Effect of variation of environmental conditions on the microbial communities of deep-sea vent chimneys cultured in a bioreactor. *Extremophiles*, **13**: 595-608.
- Colodner D., Lin J., Von Damm K., Buttermore L., Kozlowski R., Charlou J.-L., Donval J.P. & Wilson C. 1993.** Chemistry of the Lucky Strike hydrothermal fluids: initial results. *Eos, Transactions, American Geophysical Union*, **99**.
- Comtet T., Jollivet D., Khripounoff A., Segonzac M. & Dixon D.R. 2000.** Molecular and morphological identification of *Bathymodiolus azoricus* (Bivalvia: Mytilidae) *in situ*-preserved in sediment traps at Rainbow hydrothermal vent field (Mid-Atlantic Ridge). *Limnology and Oceanography*, **45**: 1655-1661.
- Desbruyères D., Biscoito M., Caprais J.C., Colaço A., Comtet T., Crassous P., Fouquet Y., Khripounoff A., Le Bris N., Olu K., Sarradin P.M., Segonzac M. & Vangriesheim A. 2001.** Variations in deep-sea hydrothermal vent communities on the Mid-Atlantic Ridge when approaching the Azores plateau. *Deep-Sea Research 1*, **48**: 1325-1346.
- Dymond J. & Roth S. 1988.** Plume dispersed hydrothermal particles: A time-series record of settling flux from the Endeavour Ridge using moored sensors. *Geochimica et Cosmochimica Acta*, **52**: 2525-2536.
- Elderfield H. & Schultz A. 1996.** Mid-ocean ridge hydrothermal fluxes and the chemical composition of the ocean. *Annual Review of Earth and Planetary Sciences*, **24**: 191-224.
- Erauso G., Reysenbach A. L., Godfroy A., Meunier J. R., Crump B., Partensky F., Baross J.A., Marteinson V, Barbier G, Pace N.R. & Prieur D. 1993.** *Pyrococcus abyssi* sp. nov. , a new hyperthermophilic archaeon isolated from a deep-sea hydrothermal vent. *Archives of Microbiology*, **160**:338-349.
- Flores G.E., Campbell J.H., Kirshtein J.D., Meneghin J., Podar M., Steinberg J.I., Seewald J.S., Tivey M. K., Voytek M. A., Yang Z. K. & Reysenbach A.-L. 2011.** Microbial community structure of hydrothermal deposits from geochemically different vent fields along the Mid-Atlantic Ridge. *Environmental Microbiology*, **13**: 2158-2171
- Haouari O., Fardeau M.-L., Cayol J.-L., Casiot C., Elbaz-Poulichet F., Hamdi M., Joseph M. & Ollivier B. 2008.** *Desulfotomaculum hydrothermale* sp. nov., a thermophilic sulfate-reducing bacterium isolated from a terrestrial Tunisian hot spring. *International Journal of Systematic and Evolutionary Microbiology*, **58**: 2529-2535.
- Herring P.J. & Dixon D.R. 1998.** Extensive deep-sea dispersal of postlarval shrimp from a hydrothermal vent. *Deep-Sea Research 1*, **45**: 2105-2118.
- Huber R., Stoffers P., Cheminee J.L., Richnow H.H. & Stetter K.O. 1990.** Hyperthermophilic archaeobacteria within the crater and open sea plume of erupting Macdonald seamount. *Nature*, **345**: 179-182.
- Kaksonen A.H., Plumb J.J., Robertson W.J., Spring S., Schumann P., Franzmann P.D. & Puhakka J.A. 2006.** Novel Thermophilic Sulfate-Reducing Bacteria from a Geothermally Active Underground Mine in Japan. *Applied and Environmental Microbiology*, **72**: 3759-3762.
- Khripounoff A., Comtet T., Vangriesheim A. & Crassous P. 2000.** Near-bottom biological and mineral particle flux in the Lucky Strike hydrothermal vent area (Mid-Atlantic Ridge). *Journal of Marine Systems*, **25**: 101-118.
- Khripounoff A., Vangriesheim A., Crassous P., Segonzac M., Colaço A., Desbruyères D. & Barthelemy R. 2001.** Particle flux in the Rainbow hydrothermal vent field (Mid-Atlantic Ridge): Dynamics, mineral and biological composition. *Journal of Marine Research*, **59**: 633-656.
- Khripounoff A., Vangriesheim A., Crassous P., Segonzac M., Lafon V. & Warén A. 2008.** Temporal variation of currents, particulate flux and organism supply at two deep-sea hydrothermal fields of the Azores Triple Junction. *Deep-Sea Research 1*, **55**: 532-551.

- Kim S.L. & Mullineaux L.S. 1998.** Distribution and near-bottom transport of larvae and other plankton at hydrothermal vents. *Deep-Sea Research 2*, **45**: 423-440.
- Langmuir C., Charlou J.L., Colodner D., Corey S., Costa I., Desbruyères D., Desonie D., Emerson T., Fornani D., Fouquet Y., Humphris S., Fiala-Medioni A., Saldanha L., Sours-Page R., Thatcher M., Tivey M.K., Van Dover C., Von Damm K., Wiese K. & Wilson C. 1993.** Lucky Strike: A newly discovered hydrothermal site on the Azores platform. *RIDGE Events*, **4**: 3-5.
- Marsh A.G., Mullineaux L.S., Young C.M. & Manahan D.T. 2001.** Larval dispersal potential of the tubeworm *Riftia pachyptila* at deep-sea hydrothermal vents. *Nature*, **411**: 77-80.
- McCliment E.A., Voglesonger K.M., O'Day P.A., Dunn E.E., Holloway J.R., Cary & S.C. 2006.** Colonization of nascent, deep-sea hydrothermal vents by a novel Archaeal and Nanoarchaeal assemblage. *Environmental Microbiology*, **8**: 114-125.
- Metaxas A., 2004.** Spatial and temporal patterns in larval supply at hydrothermal vents in the northeast Pacific Ocean. *Limnology and Oceanography*, **49**: 1949-1956.
- Mullineaux L.S. & France S.C. 1995.** Dispersal mechanisms of deep-sea hydrothermal vent fauna. In S.E. Humphris, R.A. Zierenberg, L.S. Mullineaux, R.E. Thomson, *Seafloor hydrothermal systems: physical, chemical, biological, and geological interactions*, Vol. Geophysical Monograph 91 (pp. 408-424). Washington: American Geophysical Union.
- Mullineaux L.S., Mills S.W., Sweetman A.K., Beaudreau A.H., Metaxas A. & Hunt H.L. 2005.** Vertical, lateral and temporal structure in larval distributions at hydrothermal vents. *Marine Ecology Progress Series*, **293**: 1-16.
- Postec A., Lesongeur F., Pignet P., Ollivier B., Quérellou J. & Godfroy A. 2007.** Continuous enrichment cultures: insights into prokaryotic diversity and metabolic interactions in deep-sea vent chimneys. *Extremophiles*, **11**: 747-757.
- Postec A., Pignet P., Cuff-Gauchard V., Schmitt A., Querellou J. & Godfroy A. 2005.** Optimisation of growth conditions for continuous culture of the hyperthermophilic archaeon *Thermococcus hydrothermalis* and development of sulphur-free defined and minimal media. *Research in Microbiology*, **156**: 82-87
- Roussel E., Cambon-Bonavita M., Querellou J., Cragg B.A., Webster G., Prieur D. & Parkes R.J. 2008.** Extending the sub-seafloor biosphere. *Science*, **320**: 1046.
- Schrenk M.O., Kelley D.S., Delaney J.R. & Baross J.A. 2003.** Incidence and Diversity of Microorganisms within the Walls of an Active Deep-Sea Sulfide Chimney. *Applied and Environmental Microbiology*, **69**: 3580-3592.
- Webster G, Newberry C. J., Fry J. C. & Weightman. A.J. 2003.** Assessment of bacterial community structure in the deep sub-seafloor biosphere by 16s rDNA-based techniques: a cautionary tale. *Journal of Microbiological Methods*, **55**: 155-164.
- Wery N., Cambon-Bonavita M.-A., Lesongeur F. & Barbier G. 2002.** Diversity of anaerobic heterotrophic thermophiles isolated from deep-sea hydrothermal vents of the Mid-Atlantic Ridge. *FEMS Microbiology Ecology*, **41**: 105-114.
- Wery N., Moricet J.-M., Cuff V., Pignet P., Lesongeur F., Cambon-Bonavita M.-A. & Barbier G. 2001.** *Caloranaerobacter azorensis* gen. nov., sp. nov., an anaerobic thermophilic bacterium isolated from a deep-sea hydrothermal vent. *International Journal of Systematic and Evolutionary Microbiology*, **51**: 1789-1796.

## Tables

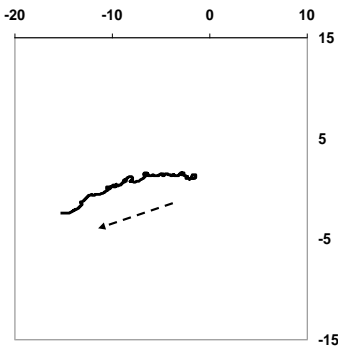
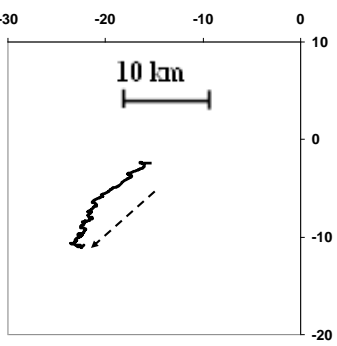
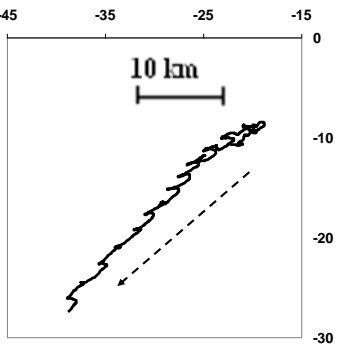
**Table 1.** Main current speed and direction, progressive vector diagram and percentage of temperature anomalies during the different particle sampling periods measured at the base of the Tour Eiffel hydrothermal vent.

**Tableau 1.** Vitesse et direction du courant, hodographe intégré et pourcentage d'anomalies de température pendant la durée les prélèvements de particules au pied de la source hydrothermale Tour Eiffel.

(a) At the base of the vent	Sample 1	Sample 2	Sample 3
Sampling period	31/07/2005- 06/08/2005	07/08/2005- 13/08/2005	14/08/2005-23/08/2005
Mean current speed and direction Progressive vector diagram of the current	5.2 cm s <sup>-1</sup> –north and southeast	5.0 cm s <sup>-1</sup> - southeast and north	6.6 cm s <sup>-1</sup> - southeast
			
% of temperature anomalies (> 4.5°C)	9.3	18.2	27.1

**Table 2.** Main current directions, progressive vector diagram and percentage of temperature anomalies during the different particle sampling periods measured at 1000m to the hydrothermal vent tour Eiffel.

**Tableau 1.** Vitesse et direction du courant, hodographe intégré et pourcentage d'anomalies de température pendant la durée les prélèvements de particules à 1000 m de la cheminée hydrothermale Tour Eiffel.

At 1000m south of the vent	Sample 1	Sample 2	Sample 3
<b>Sampling period</b>	31/07/2005- 06/08/2005	07/08/2005- 13/08/2005	14/08/2005-23/08/2005
<b>Mean current speed and direction Progressive vector diagram of the current</b>	 <p>3.9 cm s<sup>-1</sup> - east-west</p>	<p>3.8 cm s<sup>-1</sup> - north southwest</p>  <p>10 km</p>	<p>6.5 cm s<sup>-1</sup> - northeast- SOU</p>  <p>10 km</p>
<b>% of temperature anomalies (&gt; 4.5°C)</b>	<p>10 km</p> <p>No anomalies</p>	No anomalies	No anomalies

**Table 3.** Results of enrichments cultures from particles sampled with sediment traps.

**Tableau 3.** Résultats des cultures d'enrichissements des particules échantillonnées avec les pièges à particules

Trap sample	SME 90°C	GYPS sulfur 60°C	GYPS thiosulfate 60°C
TS	+++ <sup>a</sup>	+++ <sup>a</sup>	+++ <sup>a</sup>
T100	+++ <sup>a</sup>	+++ <sup>b</sup>	+++ <sup>b</sup>
T300	+++ <sup>b</sup>	+++ <sup>a</sup>	+ <sup>a, b</sup>
T1000	+++ <sup>b</sup>	-	-

(+++ >10<sup>8</sup> cells.ml<sup>-1</sup> (final concentration); ++ 2x10<sup>7</sup> to 10<sup>8</sup>; + <2x10<sup>7</sup>  
Culture (<sup>a</sup>) after 16 hours, (<sup>b</sup>) after 24 hours.

**Table 4.** Microbial species enriched in the four sediment traps (enrichment media in parentheses)

**Tableau 4.** Espèces microbiennes retrouvées dans les 4 pièges à particules (entre parenthèse, les milieu de culture)

Trap sample	Detected species
TS	<i>Thermococcus</i> sp. (SMEYP and GYPS sulfur) <i>Caloranaerobacter</i> sp.(GYPS sulfur or thiosulfate)
T100	<i>Thermococcus</i> sp. (SMEYP and GYPS sulfur) <i>Desulfotomaculum</i> sp. (GYPS sulfur) <i>Caminicella</i> sp. (GYPS sulfur or thiosulfate)
T300	<i>Thermococcus</i> sp. ((SMEYP and GYPS sulfur) <i>Caloranaerobacter</i> sp. (GYPS sulfur or thiosulfate)
T1000	<i>Thermococcus</i> sp. (SMEYP)

**Table 5.** Faunal composition of samples from the four sediment traps.

**Tableau 5.** Composition faunistique des échantillons récoltés par les quatre pièges à particules

<b>Trap</b>	<b>Origin</b>	<b>Fauna</b>	<b>31/7-6/8</b>	<b>7/8-13/8</b>	<b>14/8-24/8</b>	<b>Total</b>
<b>TS</b>	Hydrothermal	Postlarvae	4	10	1	15
		bivalve	3	4	3	10
	pelagic	Gastropods				
		Polychaetes	4	12	8	24
		Copepods	0	7	5	12
	Other	1	1	2	4	
<b>T100</b>	Hydrothermal	Postlarvae	1			1
		bivalve				0
		Gastropods				
	Pelagic	Polychaetes				0
		Copepods	2	6	5	13
	Other			4	4	
<b>T300</b>	Hydrothermal	Postlarvae				0
		bivalve				0
		Gastropods				
	Pelagic	Polychaetes	1			1
		Copepods		2	1	3
	Other	3		1	4	
<b>T1000</b>	Hydrothermal	Postlarvae		1		1
		bivalve				0
		Gastropods				
	Pelagic	Polychaetes	1	1		2
		Copepods	7	6	5	18
	Other	3	2	4	9	

## Figures

**Figure 1.** Map of the Lucky Strike vent site with the mooring locations and the photo of the sediment trap *in situ* close to the Eiffel Tower chimney

**Figure 1.** Carte du site hydrothermal Lucky Strike avec les positions des mouillages et la photo du piège à particules *in situ* déposé au pied de la cheminée Tour Eiffel.

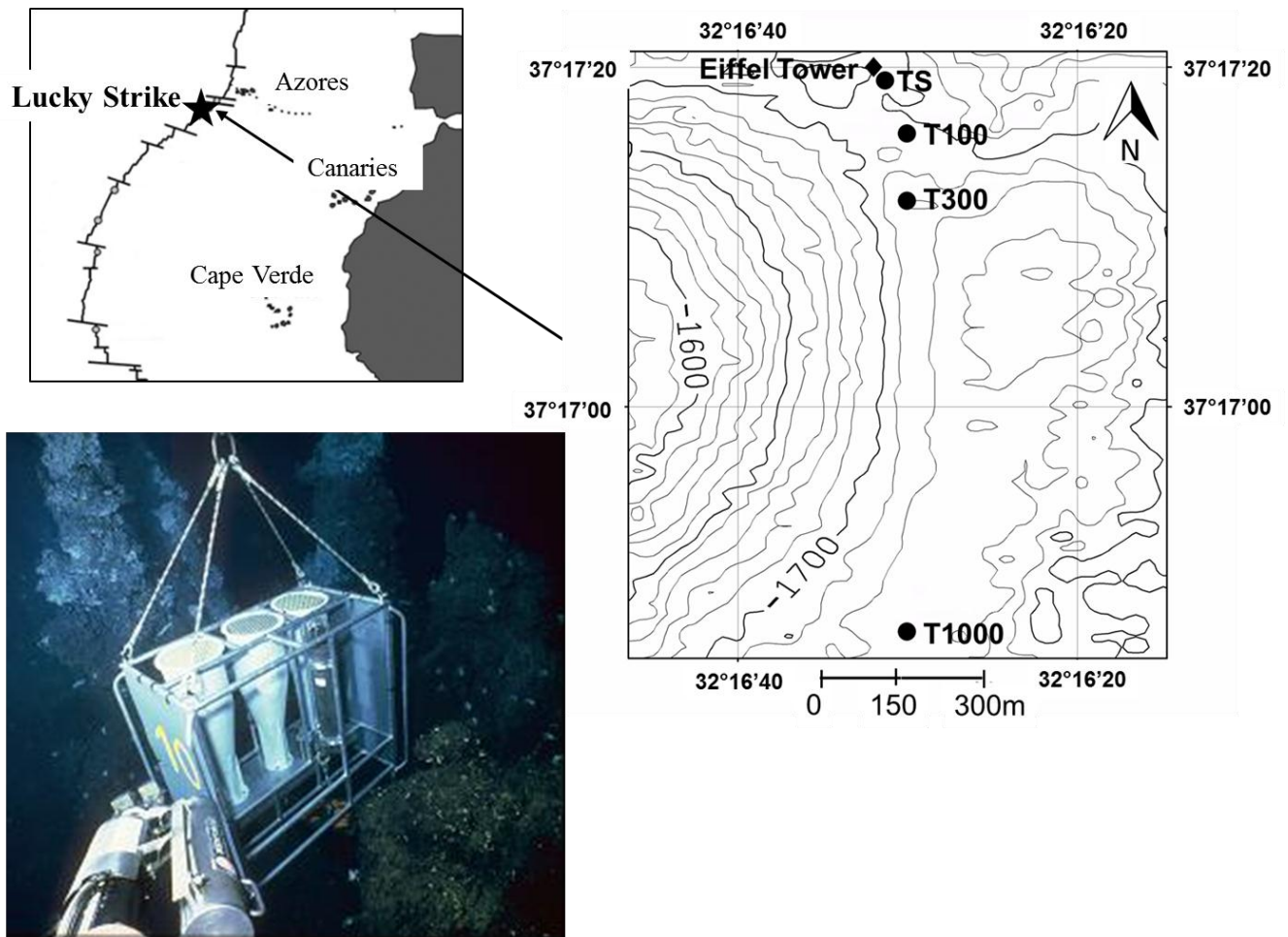


**Figure 2.** Temperature versus current direction recorded at the base of the Eiffel Tower hydrothermal vent

**Figure 2.** Relation entre la température et la direction du courant enregistré au pied de la cheminée Tour Eiffel

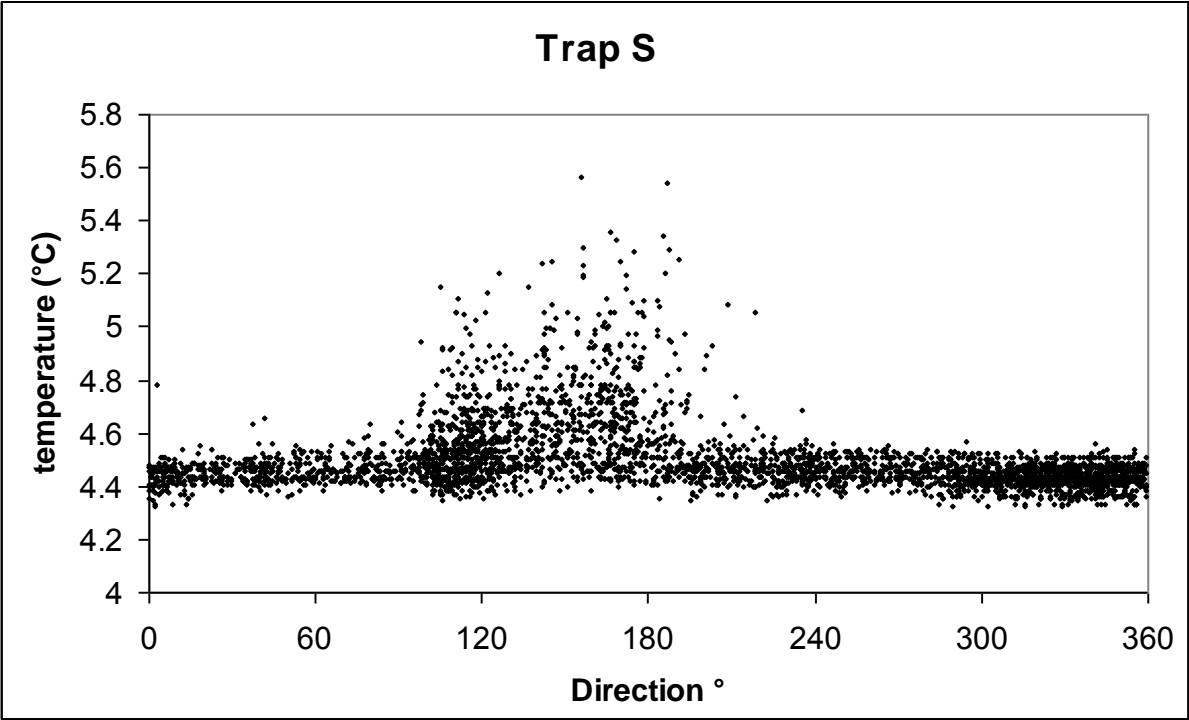


**Figure 3.** Variation of particle flux according to distance from the hydrothermal chimney (dotted line shows expected values based on a power regression model)

**Figure 3.** Variation du flux particulaire en fonction de la distance à la cheminée (la courbe en pointillée indique le résultat attendu à partir d'un modèle de régression de puissance)

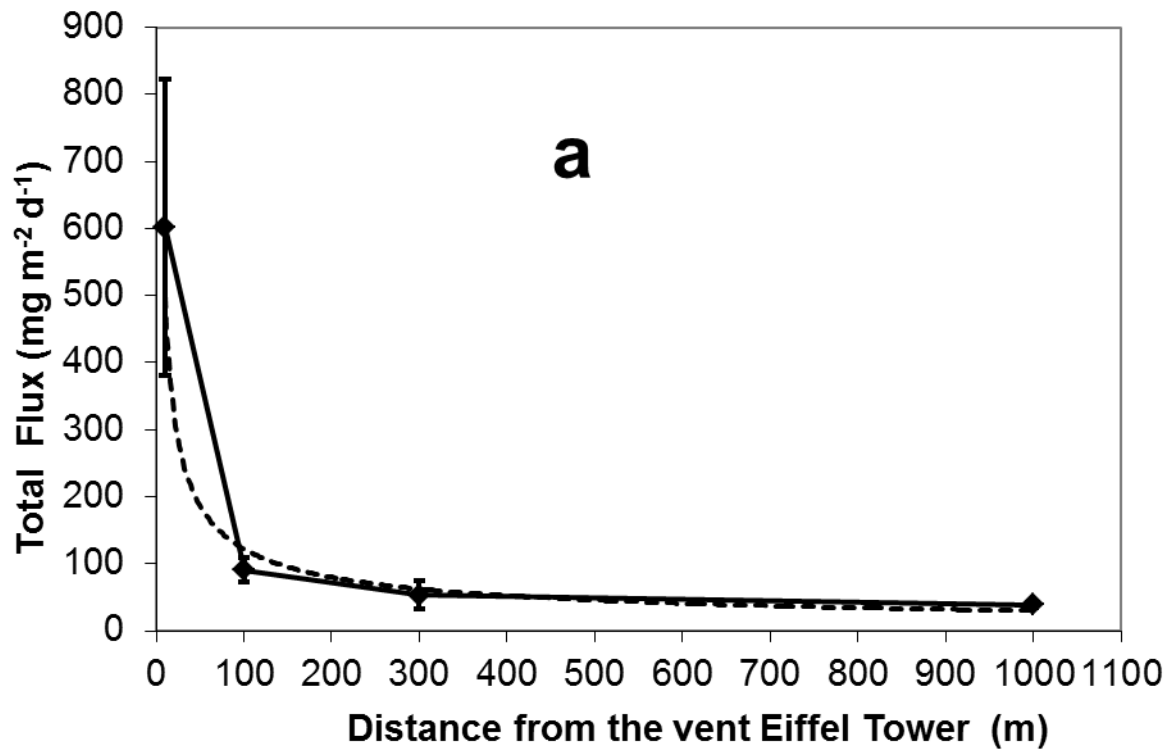


**Figure 4.** Temporal variation in particle flux for the four sediment traps recorded during the sampling periods. The percentage of temperature anomalies is given in parentheses (see text). Polar representations indicate the main direction of the current during the temperature anomaly periods.

**Figure 4.** Variation temporel du flux particulaire dans les quatre pièges à particules enregistrée pendant les différentes périodes d'échantillonnages. Le pourcentage d'anomalies de température est indiqué entre parenthèse (voir texte). Les représentations polaires montrent la direction principale du courant pendant l'apparition des anomalies de température.

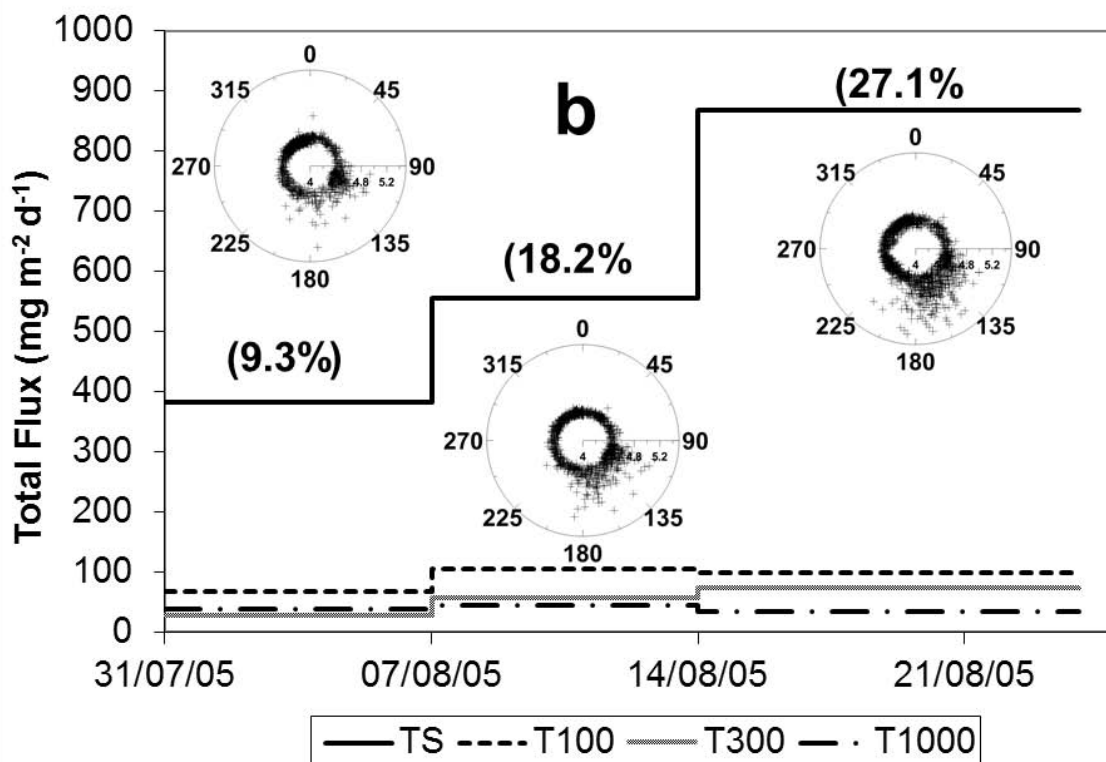


**Figure 5.** Elemental composition (A) and flux (B) of particle sampled at various distances from the Eiffel Tower vent site

**Figure 5.** Composition élémentaire (A) et flux (B) des particules échantillonnées par les pièges à différentes distances de la cheminée Tour Eiffel.

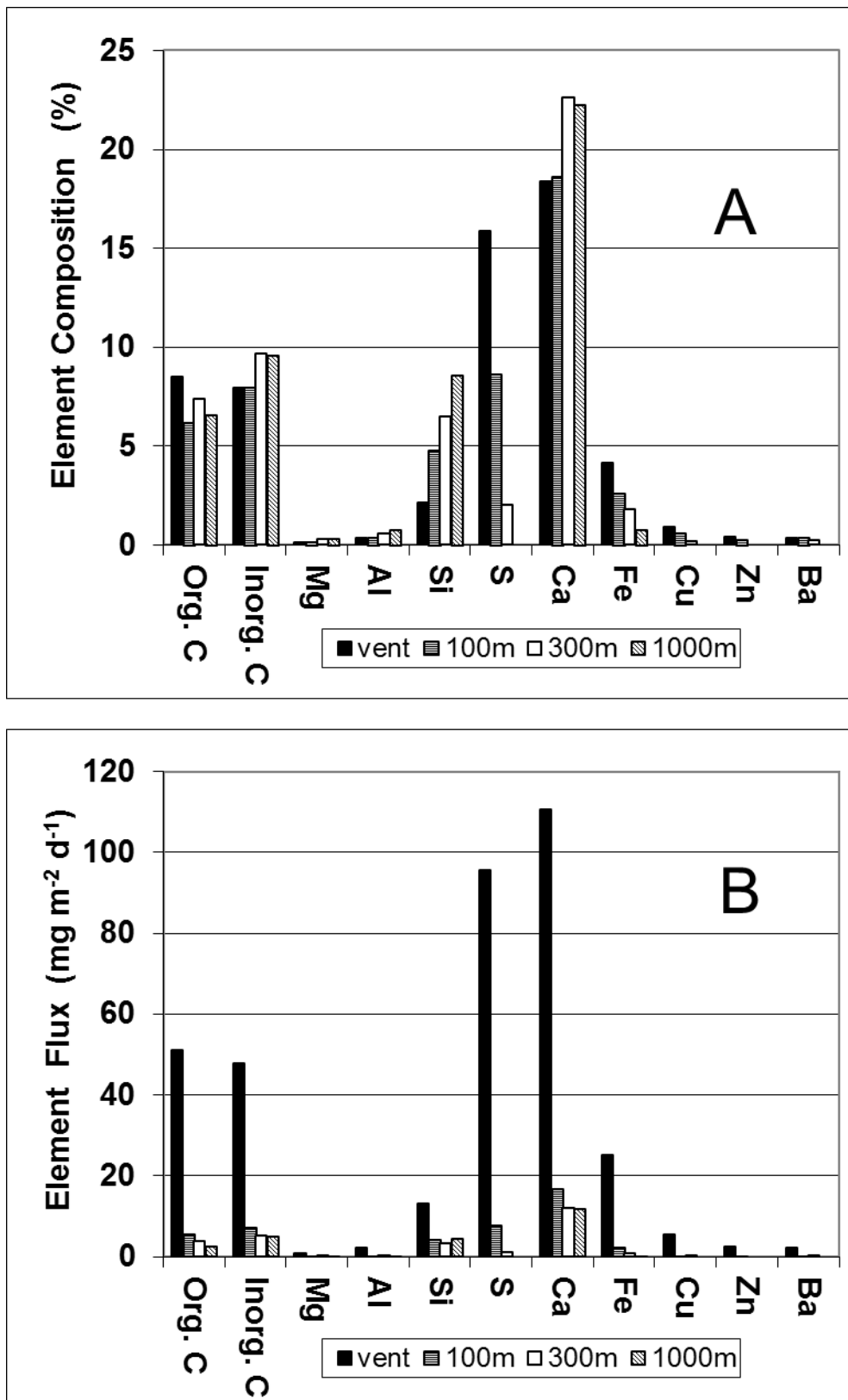


**Figure 6.** Trends in particle flux and organic carbon concentration in the TS sediment trap close to the hydrothermal chimney during the study period

**Figure 6.** Evolution du flux particulaire et de la concentration en carbone organique dans le piège à particules TS au pied de la cheminée hydrothermale pendant la durée de l'expérience.

